

SCIENTIFIC REPORTS



OPEN

Calcium Channels and Oxidative Stress Mediate a Synergistic Disruption of Tight Junctions by Ethanol and Acetaldehyde in Caco-2 Cell Monolayers

Received: 01 August 2016
Accepted: 14 November 2016
Published: 13 December 2016

Geetha Samak*, Ruchika Gangwar*, Avtar S. Meena, Roshan G. Rao, Pradeep K. Shukla, Bhargavi Manda, Damodaran Narayanan, Jonathan H. Jaggar & Radha Krishna Rao

Ethanol is metabolized into acetaldehyde in most tissues. In this study, we investigated the synergistic effect of ethanol and acetaldehyde on the tight junction integrity in Caco-2 cell monolayers. Expression of alcohol dehydrogenase sensitized Caco-2 cells to ethanol-induced tight junction disruption and barrier dysfunction, whereas aldehyde dehydrogenase attenuated acetaldehyde-induced tight junction disruption. Ethanol up to 150 mM did not affect tight junction integrity or barrier function, but it dose-dependently increased acetaldehyde-mediated tight junction disruption and barrier dysfunction. Src kinase and MLCK inhibitors blocked this synergistic effect of ethanol and acetaldehyde on tight junction. Ethanol and acetaldehyde caused a rapid and synergistic elevation of intracellular calcium. Calcium depletion by BAPTA or Ca^{2+} -free medium blocked ethanol and acetaldehyde-induced barrier dysfunction and tight junction disruption. Diltiazem and selective knockdown of TRPV6 or $\text{Ca}_v1.3$ channels, by shRNA blocked ethanol and acetaldehyde-induced tight junction disruption and barrier dysfunction. Ethanol and acetaldehyde induced a rapid and synergistic increase in reactive oxygen species by a calcium-dependent mechanism. N-acetyl-L-cysteine and cyclosporine A, blocked ethanol and acetaldehyde-induced barrier dysfunction and tight junction disruption. These results demonstrate that ethanol and acetaldehyde synergistically disrupt tight junctions by a mechanism involving calcium, oxidative stress, Src kinase and MLCK.

A significant body of evidence indicates that alcohol consumption causes gut barrier dysfunction leading to increased endotoxin flux from the intestinal lumen into the mucosa, and eventually into the blood circulation causing the condition, “Alcoholic Endotoxemia”^{1,2}. Gut permeability and endotoxemia seem to play crucial role in the pathogenesis of alcoholic liver disease and potentially in alcoholic damage to other organs. Therefore, the loss of mucosal barrier function and increased gut permeability play a central role in the mechanism of alcoholic tissue injury. Tissues *in vivo* are simultaneously exposed to ethanol and acetaldehyde due to ubiquitous distribution of alcohol dehydrogenase (ADH)³, CYP2E1⁴ and catalase^{5,6}, all known to metabolize ethanol into acetaldehyde. Mounting evidence indicates that ethanol metabolism by ADH into acetaldehyde plays a crucial role in alcoholic tissue injury in many organs^{7–13}. Studies reported so far have evaluated the effect of either ethanol or acetaldehyde on tissue functions, including the epithelial barrier function. In the present study, we addressed the potential cross talk between ethanol and acetaldehyde in disrupting the intestinal epithelial tight junction integrity and barrier function.

Epithelial tight junctions confer the intestinal mucosal barrier function in the intestine. Tight junctions are multi protein complexes consisting of transmembrane proteins such as occludin, tricellulin, claudins and junctional adhesion molecules and adapter proteins such as ZO-1, ZO-2 and ZO-3, which interact with many other proteins including actin-binding proteins^{14–16}. Tight junction protein complexes are anchored to the actin

Department of Physiology, University of Tennessee Health Science Center, 894 Union Avenue, Memphis TN 38163, USA. *These authors contributed equally to this work. Correspondence and requests for materials should be addressed to R.K.R. (email: rrao2@uthsc.edu)

cytoskeleton¹⁵. Protein-protein interactions and the association with the actin cytoskeleton are essential for the assembly and maintenance of tight junction integrity. Many signaling molecules, including protein kinases and proteins phosphatases, interact with the tight junction proteins, and the tight junction integrity is regulated by intracellular signal transduction¹⁷.

Acetaldehyde has been shown to disrupt the intestinal epithelial tight junctions and increase paracellular permeability to endotoxins¹². Acetaldehyde inhibits protein tyrosine phosphatases and increases tyrosine phosphorylation of tight junction and adherens junction proteins^{18,19}. Acetaldehyde also induces translocation of protein phosphatase PP2A to tight junctions and dephosphorylates tight junction proteins on threonine residues²⁰. The role of ethanol metabolism into acetaldehyde in the intestinal permeability was confirmed in rat intestine *ex vivo*²¹ and mouse colon *in vivo*²². Therefore, the role of acetaldehyde in disruption of intestinal epithelial tight junction is well established. But, the direct effect of ethanol on epithelial permeability is controversial. Few studies failed to show an effect of ethanol on barrier function at concentrations lower than 2.5%^{23–26}, whereas other studies have recorded a direct effect of ethanol on the barrier function in Caco-2 cell monolayers²⁷. The simultaneous exposure of tissues to ethanol and acetaldehyde in alcoholics raises the question whether one influences the effect of other in causing tissue injury.

In the present study, we investigated the synergistic effect of ethanol and acetaldehyde on the tight junction integrity and barrier function in Caco-2 cell monolayers, and delineated the role of calcium influx and mitochondrial oxidative stress in the mechanism involved in the synergistic effect of ethanol and acetaldehyde.

Results

Ethanol metabolism plays a role in tight junction disruption and barrier dysfunction. Caco-2 cells express high level of aldehyde dehydrogenase (ALDH), but only trace level of ADH is detected²⁸. Previous studies showed that acetaldehyde is more effective than ethanol in tight junction disruption in Caco-2 cell monolayer¹. To confirm the role of ethanol metabolism on tight junction disruption Caco-2 cells were transfected with ADH1B or ALDH2. Immunoblot analysis showed only trace amount of ADH in vector-transfected cell monolayers, whereas ADH1B-transfected cells showed high level of ADH (Fig. 1A). Incubation of vector-transfected cells with ethanol up to 150 mM caused no significant effect on transepithelial electrical resistance (TER) (Fig. 1B) or inulin permeability (Fig. 1C). But, ethanol dose-dependently reduced TER and increased inulin permeability in ADH1B-transfected cell monolayers. Confocal immunofluorescence microscopy showed that ethanol produced no obvious effect on junctional distribution of occludin and ZO-1, but it caused a dramatic redistribution of occludin and ZO-1 from the intercellular junctions into intracellular compartment in ADH1B-transfected cell monolayers (Fig. 1D).

Higher level of ALDH was detected in ALDH2-transfected cells compared to that in vector-transfected cells (Fig. 1E). Incubation with acetaldehyde induced dose-dependent decrease in TER (Fig. 1F) and increase in inulin permeability (Fig. 1G), and these effects were significantly dampened in ALDH2-transfected cell monolayers. Acetaldehyde-induced redistribution of occludin and ZO-1 from the intercellular junctions was also diminished in ALDH2-transfected cell monolayers compared to that in vector-transfected cell monolayers (Fig. 1H).

Ethanol synergizes acetaldehyde-induced tight disruption and barrier dysfunction. To determine the influence of ethanol on acetaldehyde effect we evaluated acetaldehyde-induced barrier dysfunction and tight junction disruption in the presence of varying concentrations of ethanol. In the absence of acetaldehyde, ethanol up to 150 mM showed no significant effect on TER (Fig. 2A). In the absence of ethanol, acetaldehyde at 100 μ M and 200 μ M concentrations reduced TER by 20% and 50%, respectively. These effects of acetaldehyde on TER were dose-dependently elevated by ethanol (Fig. 2A). Similarly, ethanol in the absence of acetaldehyde produced no significant effect on inulin permeability. In the absence of ethanol, acetaldehyde at 100 μ M concentration produced no significant effect on inulin permeability, and produced only slight increase in inulin permeability at 200 μ M concentration (Fig. 2B). Acetaldehyde effect on inulin permeability at both 100 μ M and 200 μ M concentrations were dose-dependently elevated by ethanol. Immunofluorescence images show that ethanol in the absence of acetaldehyde caused no obvious effect on junctional distribution of occludin and ZO-1, but acetaldehyde (200 μ M) in the absence of ethanol showed a partial depletion of junctional organization of occludin and ZO-1 (Fig. 2C). Acetaldehyde in the presence of ethanol caused a dramatic redistribution of occludin and ZO-1 from the intercellular junctions into intracellular compartments (Fig. 2C).

To determine the signaling mechanism associated with the synergistic effect of ethanol and acetaldehyde we evaluated the effect of Src kinase inhibitor (PP2) and myosin light chain kinase (MLCK) inhibitor (ML-7). Both PP2 and ML-7 significantly blocked ethanol and acetaldehyde-induced decrease in TER (Fig. 3A) and increase in inulin permeability (Fig. 3B). Immunofluorescence images show that both PP2 and ML-7 blocked ethanol and acetaldehyde-induced redistribution of occludin and ZO-1 from the intercellular junctions (Fig. 3C). Previous studies showed that acetaldehyde at higher concentration (400 μ M) causes barrier dysfunction in the absence of ethanol. We evaluated the effect of PP2 and ML-7 on the effect of higher dose of acetaldehyde. Acetaldehyde increased inulin permeability by several folds, but PP2 or ML-7 failed to block this effect of acetaldehyde (Fig. 3D).

Ethanol and acetaldehyde synergistically elevate intracellular calcium ($[Ca^{2+}]_i$) leading to tight junction disruption. The effect of ethanol and acetaldehyde on $[Ca^{2+}]_i$ was evaluated by live cell fluorescence imaging. Application of ethanol alone up to 1% concentration produced no significant effect on $[Ca^{2+}]_i$ at least up to 30 min. Similarly, acetaldehyde alone up to 400 μ M caused no significant change in $[Ca^{2+}]_i$ (Fig. 4A). Interestingly, application of 200 μ M acetaldehyde 10 min after ethanol (75 mM) treatment induced a rapid increase in $[Ca^{2+}]_i$, which sustained for at least 15 min. Incubation of cells in Ca^{2+} -free medium abolished ethanol and acetaldehyde-induced rise in $[Ca^{2+}]_i$ (Fig. 4A and B). Pretreatment of cells with thapsigargin (TPG)

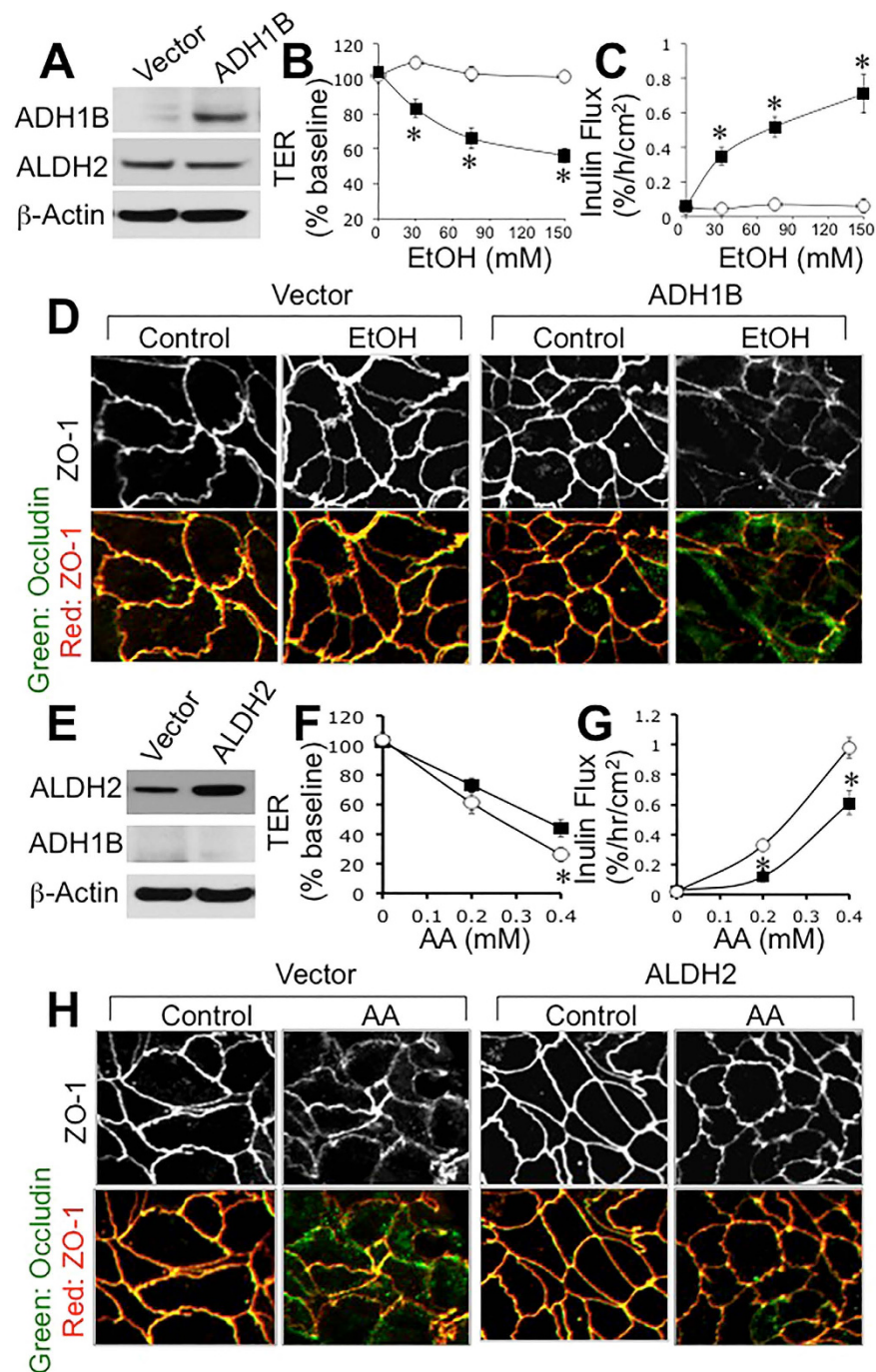


Figure 1. Expression of ADH1B and ALDH2 alters ethanol and acetaldehyde-induced tight junction disruption and barrier dysfunction. Caco-2 cells were transfected with ADH1B (closed symbols) or vector (open symbols). Expression of ADH1B in transiently transfected cells was determined by immunoblot analysis (A). Vector and ADH1B-transfected cells in transwell inserts were incubated with varying concentrations of ethanol. At 3-hour incubation, TER (B) and unidirectional flux of FITC-inulin (C) were measured. Fixed cell monolayers were stained for occludin (green) and ZO-1 (red) by immunofluorescence method (D). Values in panels B and C are mean \pm SEM (n = 6). Asterisks indicate values that are significantly (p < 0.05) different from corresponding values for control cell monolayers. Caco-2 cells were transfected with ALDH2 or vector. Expression of ALDH2 in transiently transfected cells was determined by immunoblot analysis (E). Vector (open symbols) and ALDH2 (closed symbols)-transfected cells in transwell inserts were incubated with varying concentrations of acetaldehyde. At 4-hour incubation, TER (F) and unidirectional flux of FITC-inulin (G) were measured. Fixed cell monolayers were stained for occludin (green) and ZO-1 (red) by immunofluorescence method (H). Values in panels B and C are mean \pm SEM (n = 6). Asterisks indicate values that are significantly (p < 0.05) different from corresponding values for control cell monolayers.

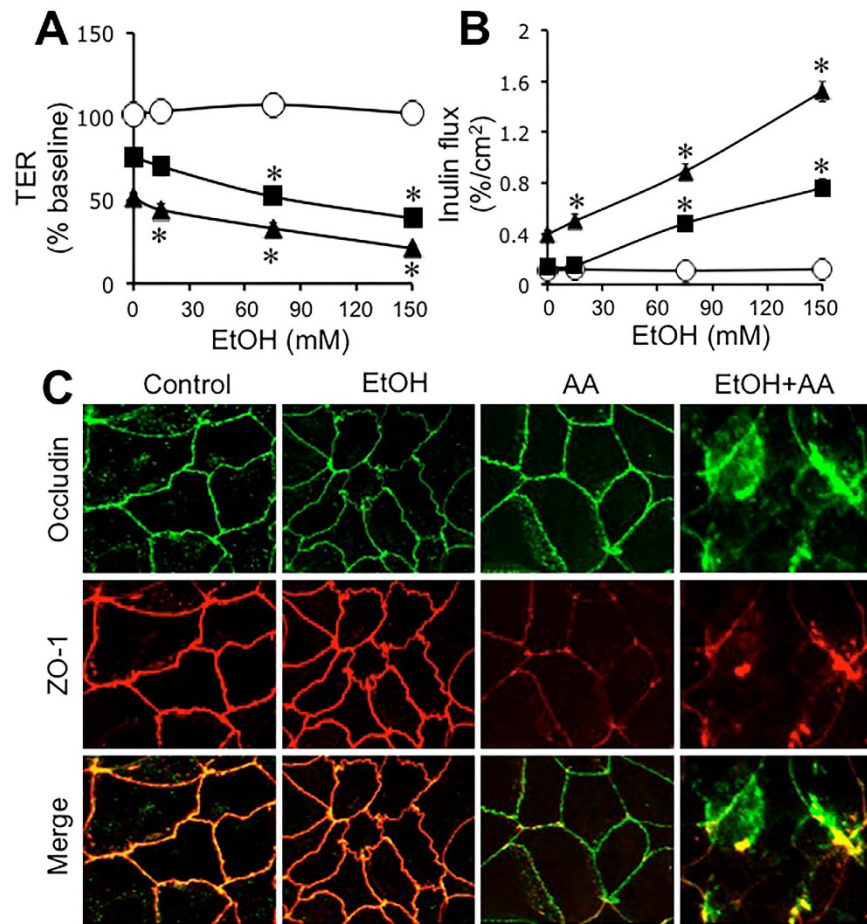


Figure 2. Ethanol and acetaldehyde induce synergistic disruption of tight junctions and barrier dysfunction. Caco-2 cells were incubated with acetaldehyde (○, 0 μM; ■, 100 μM; ▲, 200 μM) in the presence of varying concentrations of ethanol. At 4-hour incubation, TER (A) and unidirectional flux of FITC-inulin (B) were measured. Fixed cell monolayers were stained for occludin (green) and ZO-1 (red) by immunofluorescence method (C). Values are mean ± SEM (n = 6). Asterisks indicate values that are significantly (p < 0.05) different from corresponding values for control cell monolayers (without ethanol).

did not alter ethanol and acetaldehyde-induced elevation of $[Ca^{2+}]_i$. Ethanol and acetaldehyde-induced decrease in TER (Fig. 4C) and increase in inulin permeability (Fig. 4D) were blocked by BAPTA and Ca^{2+} -free medium, but not by thapsigargin (TPG). Ethanol and acetaldehyde-induced redistribution of occludin and ZO-1 from the intercellular junctions was also blocked by BAPTA and Ca^{2+} -free medium (Fig. 4E).

Ca^{2+} channels are involved in ethanol and acetaldehyde-induced tight junction disruption. To determine the role of Ca^{2+} channels we evaluated the effect of diltiazem and ruthenium red on ethanol and acetaldehyde effects. Both diltiazem and ruthenium red significantly attenuated ethanol and acetaldehyde-induced decrease in TER (Fig. 5A) and increase in inulin permeability (Fig. 5B). Diltiazem was more effective than ruthenium red in blocking the effects of ethanol and acetaldehyde. Ethanol and acetaldehyde-induced redistribution of occludin and ZO-1 from the intercellular junctions was also blocked by diltiazem (Fig. 5C). Ruthenium red caused only a partial prevention of ethanol and acetaldehyde-induced redistribution of occludin and ZO-1.

Calcium channels, $Ca_v1.3$ and TRPV6, were knocked down by specific shRNAs (Fig. 5D). Ethanol and acetaldehyde-induced decrease in TER (Fig. 5E) and increase in inulin permeability (Fig. 5F) were significantly low in $Ca_v1.3$ and TRPV6-deficient cell monolayers compared to those in control RNA-transfected cell monolayers.

Ethanol and acetaldehyde synergistically increase reactive oxygen species (ROS). Mitochondrial Ca^{2+} overload is known to induce oxidative stress²⁹. Sustained elevation of $[Ca^{2+}]_i$ raised the question whether ethanol and acetaldehyde induce ROS production. Therefore, we examined the effect of ethanol and acetaldehyde on ROS production in Caco-2 cells by live cell fluorescence imaging. Ethanol, in the absence of acetaldehyde or acetaldehyde in the absence of ethanol, failed to increase MitoSOXTM or dichlorofluorescein (DCF)-sensitive fluorescence (Fig. 6A). But, acetaldehyde and ethanol together rapidly increased MitoSOXTM and DCF-sensitive fluorescence reaching a maximum by 45 min (Fig. 6B). MitoSOXTM is specific for mitochondrial

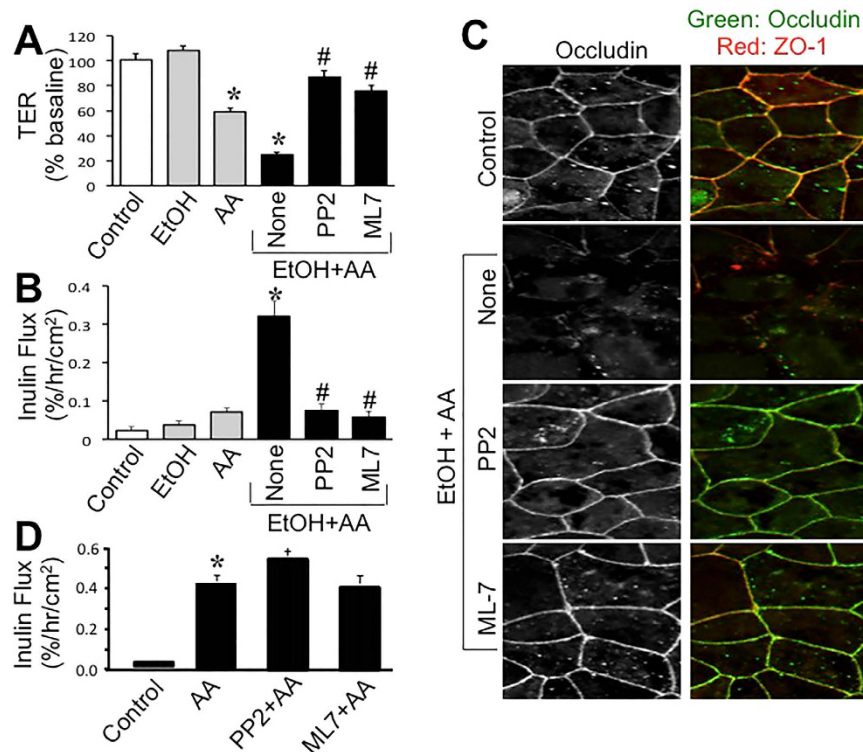


Figure 3. Src kinase and MLCK activities mediate ethanol and acetaldehyde-induced tight junction disruption and barrier dysfunction. (A–C) Caco-2 cells were preincubated with PP2 (10 μ M) or ML-7 (1 μ M) 30 min prior to incubation with acetaldehyde (200 μ M) in the presence of 75 mM ethanol. At 4-hour incubation, TER (A) and unidirectional flux of FITC-inulin (B) were measured. Fixed cell monolayers were stained for occludin (green) and ZO-1 (red) by immunofluorescence method (C). Values are mean \pm SEM (n = 6). Asterisks indicate values that are significantly different from corresponding values for control cell monolayers (without ethanol). (D) Cell monolayers were preincubated with PP2 (10 μ M) or ML-7 (1 μ M) 30 min prior to incubation with acetaldehyde (400 μ M). Inulin permeability was measured after 4-hour incubation. Values are mean \pm SEM (n = 6). Asterisk indicates the value that is significantly (p < 0.05) different from control value.

superoxide and DCF is relatively non-specific. Incubation of cells with Ca²⁺-free medium blocked ethanol and acetaldehyde-induced elevation of MitoSOXTM and DCF-sensitive fluorescence (Fig. 6C).

To determine the role of oxidative stress in ethanol and acetaldehyde-induced tight junction disruption and barrier dysfunction we evaluated the effect of antioxidants. Pretreatment of cell monolayers with N-acetyl L-cysteine (NAC) blocked ethanol and acetaldehyde-induced decrease in TER (Fig. 7A) and increase in inulin permeability (Fig. 7B). NAC also attenuated ethanol and acetaldehyde-induced redistribution of occludin and ZO-1 from the intercellular junctions (Fig. 7C). Pretreatment with diphenyleneiodonium (DPI) failed to affect ethanol and acetaldehyde-induced changes in TER, inulin flux or redistribution of occludin and ZO-1 from the intercellular junctions. On the other hand, cyclosporine A (CsA) treatment blocked ethanol and acetaldehyde-induced decrease in TER (Fig. 7A), inulin permeability (Fig. 7B) and redistribution of occludin and ZO-1 from the junctions (Fig. 7C).

Discussion

Exposure of tissues simultaneously to ethanol and acetaldehyde is a realistic scenario in alcoholics *in vivo*. However, the information we have today were derived from studies evaluating the effect of ethanol³⁰ or acetaldehyde^{1,21,23,25,26,30} alone. The present study shows that ethanol and acetaldehyde exert a synergistic effect on the intestinal epithelial barrier function in Caco-2 cell monolayers. Furthermore, this study presents evidence to the potential mechanisms involved in the synergistic effect of ethanol and acetaldehyde on epithelial barrier function.

Mounting evidence indicates that ethanol metabolism and acetaldehyde production play crucial role in ethanol-induced tight junction disruption and barrier dysfunction in the intestinal epithelium¹. Few recent studies indicated that ethanol directly increases intestinal epithelial permeability in Caco-2 cell monolayers³⁰, but our studies have consistently showed a significant resistance of Caco-2 cell monolayers to ethanol-induced barrier dysfunction¹. Although catalase and CYP2E1 are known to metabolize ethanol into acetaldehyde, ADH is the primary mechanism of ethanol metabolism³. Following the liver, gut is the organ with high expression of ADH³. Caco-2 cells however express only trace amounts of alcohol dehydrogenase (ADH)²⁸. Accordingly, previous studies showed that ethanol disrupts barrier function of Caco-2 cell monolayers only at high concentrations^{23,25,26}, whereas its metabolic product acetaldehyde was highly effective in barrier disruption¹. Immunoblot analysis in the present study confirms lack of ADH in Caco-2 cells. The present study shows that ethanol up to 150 mM

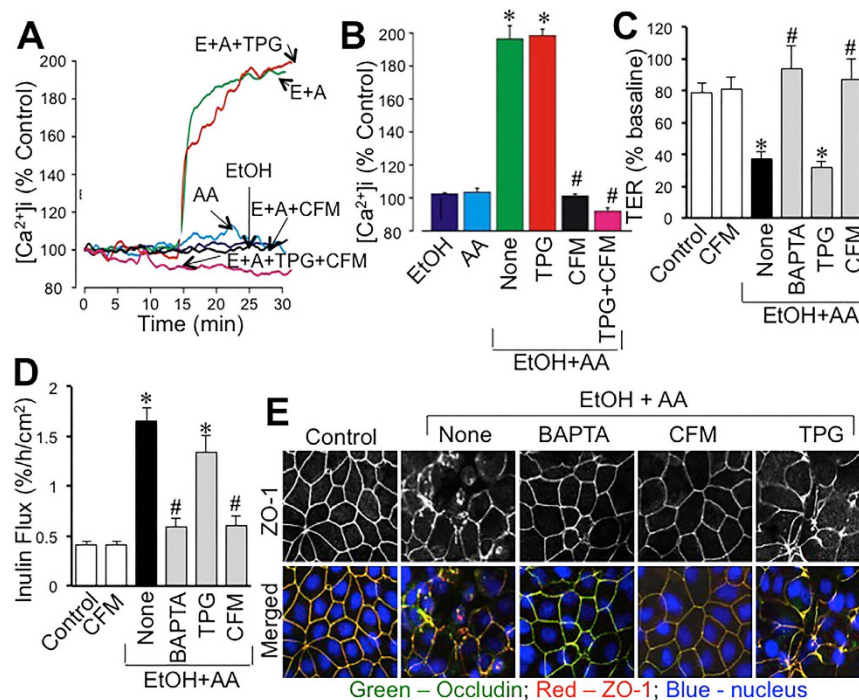


Figure 4. Synergistic elevation of intracellular Ca^{2+} by ethanol and acetaldehyde mediates tight junction disruption. (A,B) Fura-2 loaded Caco-2 cell monolayers were incubated with 75 mM ethanol (EtOH), 200 μM acetaldehyde (AA) or acetaldehyde (200 μM) added 10 min after 75 mM ethanol (E+A) in the absence or presence of thapsigargin (TPG) or Ca^{2+} -free medium (CFM). Real-time change in $[\text{Ca}^{2+}]_i$ was measured and quantitated. Values are mean \pm SEM ($n = 10$). Asterisks indicate the values that are significantly ($p < 0.05$) different from corresponding basal values; hash tags indicate values that are significantly ($p < 0.05$) different from value for E+A group. (C–E) Caco-2 cell monolayers were incubated with acetaldehyde (200 μM) added 10 min after 75 mM ethanol (EtOH+AA) in the absence (●) or presence of BAPTA-AM, TG, or CFM. Control cell monolayers received no treatments. TER (C) and inulin permeability (D) were measured after 4-hour incubation. Values are mean \pm SEM ($n = 8$). Asterisks indicate the values that are significantly different ($p < 0.05$) from corresponding control values; hash tags indicate values that are significantly different from value for “None” group (●). Cell monolayers were fixed and stained for occludin and ZO-1 (E).

concentration has no significant effect on the barrier function in Caco-2 cell monolayers. But, over expression of ADH1B increased sensitivity to ethanol-induced tight junction disruption and barrier dysfunction in Caco-2 cell monolayers, indicating that ethanol metabolism and generation of acetaldehyde is likely required for epithelial tight junction disruption. This is further confirmed by our observation that over expression of ALDH2 dampened the acetaldehyde effect on barrier function and tight junction integrity in Caco-2 cell monolayers. Variable sensitivity of Caco-2 cells for ethanol-induced tight junction disruption reported by different laboratories is possibly due to the differences in the sub clones of Caco-2 used, the passage numbers and the age of cell monolayers with different levels of ADH expression.

Due to ethanol metabolism in cells, the tissues *in vivo* are simultaneously exposed to ethanol and acetaldehyde. But, ethanol or acetaldehyde alone has been used to evaluate their effects on the intestinal epithelial barrier function in *in vitro* studies. In the present study, we show that ethanol up to 150 mM exerts no influence on barrier function in Caco-2 cell monolayers, but it dose-dependently increases the effect of acetaldehyde on barrier function and tight junction integrity. Data in Fig. 1 show that acetaldehyde is clearly required for tight junction disruption and barrier dysfunction. But, data in this figure does not rule out an influence of ethanol on the acetaldehyde-induced tight junction disruption. Data presented in Fig. 2 indicate that ethanol enhances the effect of acetaldehyde at low concentrations, although ethanol by itself shows no effect on barrier function. Acetaldehyde alone at 100 μM concentration showed no effect on inulin permeability, whereas in the presence of ethanol it significantly increased inulin permeability; this effect of ethanol was dose-dependent. These data indicate that ethanol and low concentration of acetaldehyde synergistically disrupt intestinal epithelial tight junctions and cause barrier dysfunction. It is likely that a similar synergy exists *in vivo*; acetaldehyde and ethanol are likely to cause tissue injury at concentrations lower than those reported *in vitro* studies. We evaluated the potential synergism between acetate (the product of ALDH activity) and ethanol on barrier function, but found no significant effect on barrier function. Similarly, pretreatment of cell monolayers with *E. coli* lipopolysaccharide (LPS) also had no influence on ethanol and acetaldehyde-induced barrier dysfunction.

Prevention of the ethanol and acetaldehyde-induced changes in TER, inulin permeability and redistribution of occludin and ZO-1 by PP2 indicated that Src kinase activity is involved in the synergistic effect of ethanol and acetaldehyde on barrier function and tight junction integrity. Src kinases, particularly c-Src, have been previously

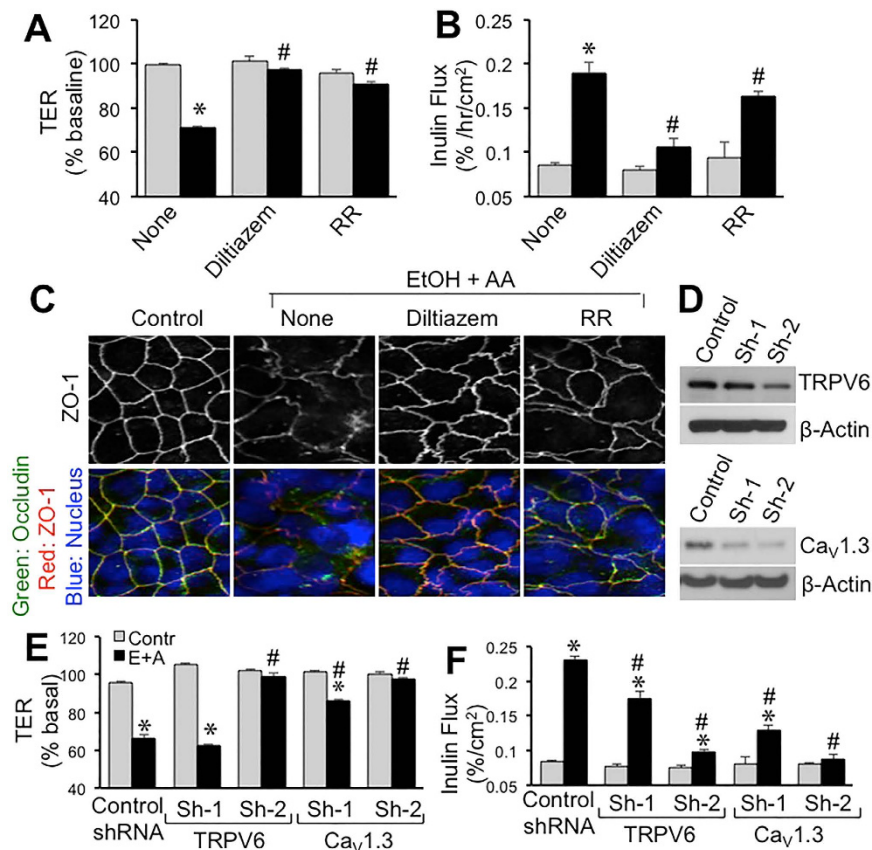


Figure 5. Ca^{2+} channels play role in ethanol and acetaldehyde-induced disruption of tight junctions and barrier dysfunction. (A–C) Caco-2 cells were preincubated with diltiazem ($30\ \mu\text{M}$) or ruthenium red (RR; $30\ \mu\text{M}$) 30 min prior to incubation with acetaldehyde ($200\ \mu\text{M}$) in the presence of $75\ \text{mM}$ ethanol (closed bars; EtOH+AA) or without acetaldehyde or ethanol treatment (gray bars). At 4-hour incubation, TER (A) and unidirectional flux of FITC-inulin (B) were measured. Fixed cell monolayers were stained for occludin (green) and ZO-1 (red) by immunofluorescence method (C). Values are mean \pm SEM ($n=6$). Asterisks indicate values that are significantly different from corresponding values for control cell monolayers (gray bars). Hash tags indicate values that are significantly different from corresponding values for “None” group. (D–F) Caco-2 cells were transfected with either of two different shRNA (Sh1 and Sh2) each for $\text{Ca}_v1.3$ and TRPV6 or control shRNA and down regulation of specific channels was confirmed by immunoblot analysis for corresponding channels (D). Transfected cell monolayers were treated with $100\ \text{mM}$ ethanol followed by $200\ \mu\text{M}$ acetaldehyde. TER (E) and inulin permeability (F) were measured. Values are mean \pm SEM ($n=6$). Asterisks indicate the values that are significantly different from corresponding control values (gray bars). Hash tags indicate values that are significantly different from corresponding values for “Control shRNA” group.

shown to mediate in tight junction disruption by hydrogen peroxide³¹, osmotic stress³² and dextran sulfate sodium³³. Tyrosine phosphorylation of tight junction proteins has been shown to prevent protein-protein interactions leading to disruption of tight junction^{34,35}. Requirement of Src kinase activity in the present study suggests that tyrosine kinases such as c-Src and tyrosine phosphorylation of tight junction proteins may be involved in the synergistic disruption of tight junction and barrier function by ethanol and acetaldehyde. Interestingly, Src kinase activity is not involved in barrier dysfunction and tight junction disruption caused by a higher concentration of acetaldehyde in the absence of ethanol. Therefore, distinct mechanisms are likely to be involved in tight junction disruption by acetaldehyde alone and the synergistic effect of ethanol and acetaldehyde. Previous studies showed that acetaldehyde increases tyrosine phosphorylation of tight junction proteins, but it was mediated by inhibition of protein tyrosine phosphatases^{18,19}.

The synergistic effect of ethanol and acetaldehyde on TER, inulin permeability and redistribution of occludin and ZO-1 was blocked by ML-7 indicating the potential role of MLCK in ethanol and acetaldehyde-induced tight junction disruption and barrier dysfunction. MLCK activity was shown to mediate the disruption of intestinal epithelial tight junction and barrier dysfunction by $\text{TNF}\alpha$ ^{36–38} and hydrogen peroxide³⁹. The original study by Ma and coworkers showed that tight junction disruption by higher concentration of ethanol in Caco-2 cell monolayers was mediated by MLCK²³.

A recent study showed a potential role of $[\text{Ca}^{2+}]_i$ in ethanol-induced tight junction disruption²⁷. MLCK activity is known to be regulated by $[\text{Ca}^{2+}]_i$. Therefore, we examined the effect of ethanol and acetaldehyde on $[\text{Ca}^{2+}]_i$. Interestingly, acetaldehyde applied following ethanol treatment rapidly increased $[\text{Ca}^{2+}]_i$ and sustained for at least

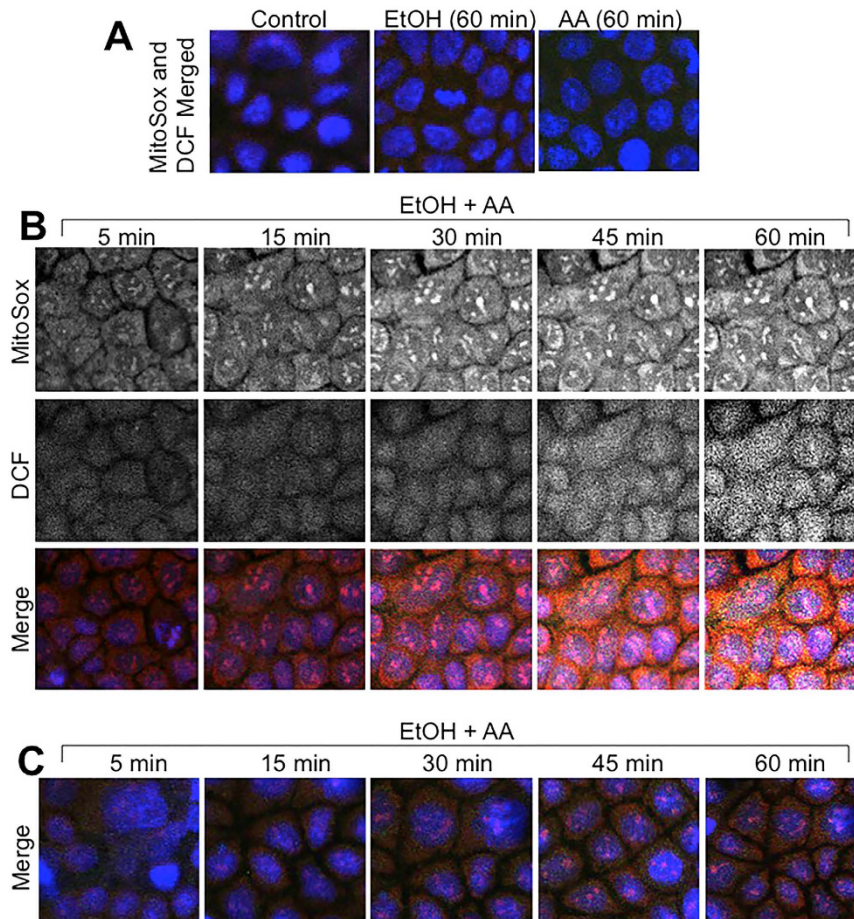


Figure 6. Ethanol and acetaldehyde induces a synergistic production of ROS by a Ca^{2+} -dependent mechanism. MitoSOXTM and H₂DCF-DA-loaded Caco-2 cell monolayers were incubated with 75 mM ethanol (EtOH) or 200 μM acetaldehyde (AA) (A) or acetaldehyde (200 μM) added 10 min after 75 mM ethanol (EtOH+AA) in the absence (B) or presence (C) of Ca^{2+} -free medium. Real-time change in $[\text{Ca}^{2+}]_i$ was imaged at varying times.

15 min. This observation indicates that ethanol and acetaldehyde synergistically elevates $[\text{Ca}^{2+}]_i$. To determine the source of elevated $[\text{Ca}^{2+}]_i$, we evaluated the effect of Ca^{2+} -free medium and TPG. A complete attenuation of ethanol and acetaldehyde-mediated elevation of $[\text{Ca}^{2+}]_i$ by Ca^{2+} -free medium indicates that influx of extracellular Ca^{2+} is involved in ethanol and acetaldehyde-induced elevation of $[\text{Ca}^{2+}]_i$. The lack of an effect of TPG indicates that Ca^{2+} release from endoplasmic reticulum is not involved in the effect of ethanol and acetaldehyde on $[\text{Ca}^{2+}]_i$ on tight junction integrity. Elevation of $[\text{Ca}^{2+}]_i$ raised the question whether $[\text{Ca}^{2+}]_i$ is involved in the synergistic disruption of tight junction by ethanol and acetaldehyde. Depletion of $[\text{Ca}^{2+}]_i$ by BAPTA or incubation in Ca^{2+} -free medium abrogated ethanol and acetaldehyde-induced barrier dysfunction and tight junction disruption. These results demonstrate that elevation of $[\text{Ca}^{2+}]_i$ plays a key role in the synergistic effect of ethanol and acetaldehyde on tight junction integrity and barrier function.

The role of Ca^{2+} influx in ethanol and acetaldehyde-induced elevation of $[\text{Ca}^{2+}]_i$ raised the question whether Ca^{2+} channels such as $\text{Ca}_v1.3$ and TRPV are involved in ethanol and acetaldehyde-induced barrier dysfunction. The results of our present study show that diltiazem, the voltage-gated channel blocker, attenuates the synergistic effect of ethanol and acetaldehyde on TER, inulin permeability and redistribution of occludin and ZO-1. This observation indicates that voltage-gated Ca^{2+} channels are involved in the disruption of tight junction and barrier dysfunction by ethanol and acetaldehyde. Ruthenium red, a selective blocker of TRPV channels and ryanodine receptors produced a partial block of the synergistic effect of ethanol and acetaldehyde on barrier function and tight junction integrity. The ruthenium red effects suggest that TRPV type of Ca^{2+} channels may also be involved in ethanol and acetaldehyde-induced tight junction disruption and barrier dysfunction. $\text{Ca}_v1.3$ and TRPV6 are two of the voltage-gated Ca^{2+} channels located in the apical membrane of intestinal epithelium. Specific knock-down of these channels by shRNA transfection in Caco-2 cells showed that both these channels are required for ethanol and acetaldehyde-induced barrier dysfunction.

To further elaborate the mechanism of synergistic effects of ethanol and acetaldehyde on tight junction and barrier function, we investigated the potential role of oxidative stress in ethanol and acetaldehyde effects. Previous studies have demonstrated that oxidative stress disrupts intestinal epithelial tight junction by activating

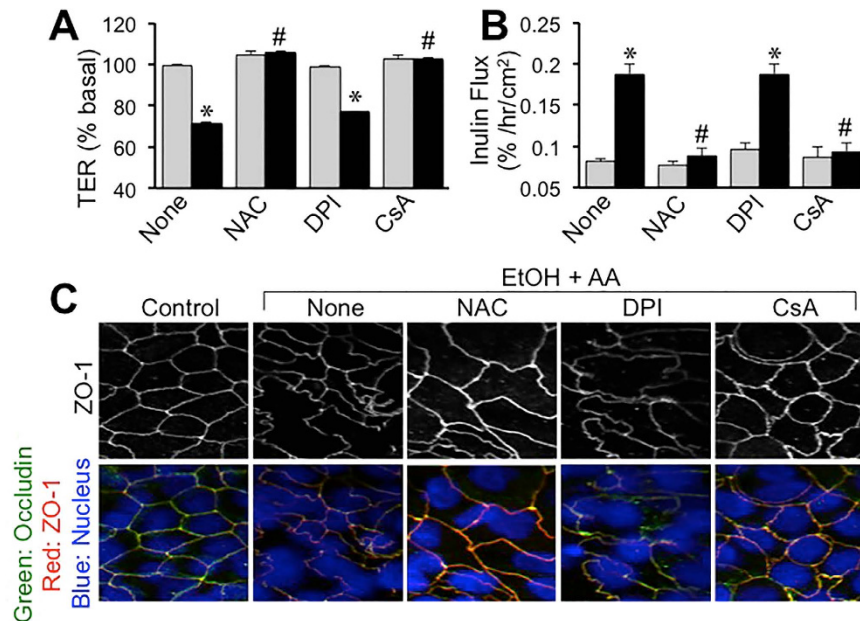


Figure 7. Oxidative stress mediates ethanol and acetaldehyde-induced tight junction disruption and barrier dysfunction. Caco-2 cells were preincubated with NAC (10 mM), DPI (10 μ M) or CsA (5 μ M) 30 min prior to incubation with acetaldehyde (200 μ M) in the presence of 75 mM ethanol (closed bars; EtOH+AA) or without acetaldehyde or ethanol treatment (gray bars). At 4-hour incubation, TER (A) and unidirectional flux of FITC-inulin (B) were measured. Fixed cell monolayers were stained for occludin (green) and ZO-1 (red) by immunofluorescence method (C). Values are mean \pm SEM (n = 6). Asterisks indicate values that are significantly different from corresponding values for control cell monolayers (gray bars). Hash tags indicate values that are significantly different from corresponding values for “None” group.

Src kinase³¹. Elevation of $[Ca^{2+}]_i$ is known to induce mitochondrial oxidative stress⁴⁰. The present study shows that ethanol or acetaldehyde alone does not induce ROS production in Caco-2 cells. However, when the acetaldehyde was applied after ethanol treatment there was a rapid and time-dependent increase in the levels of both MitoSox-sensitive and DCF-sensitive ROS. A maximum level of ROS produced was achieved by 30–45 min. MitoSox-sensitive ROS production is known to represent superoxide⁴¹, whereas DCF-sensitive ROS represent most types of ROS, including hydrogen peroxide and hydroxyl radicals⁴². The results of present study indicate that ethanol and acetaldehyde synergistically induce ROS production in Caco-2 cells, which is parallel to synergistic effect of ethanol and acetaldehyde on barrier function and $[Ca^{2+}]_i$. Prevention of ethanol and acetaldehyde-induced ROS by Ca^{2+} -free medium indicates that the elevation of $[Ca^{2+}]_i$ plays a crucial role in ethanol and acetaldehyde-induced ROS production. Ethanol and acetaldehyde-induced ROS production was also blocked by CsA. CsA is an inhibitor of mitochondrial membrane permeability transition (MMPT)⁴³, suggesting that MMPT is likely involved in ROS production. We measured the levels of NAD and NADH in cell monolayers treated with ethanol and acetaldehyde. The data show that ethanol and acetaldehyde treatment did increase NADH and NADH/NAD ratio, and the effect was maintained to be higher in ADH1B-transfected cells (Fig. S2).

Synergistic production of ROS raised the question whether oxidative stress played a role in ethanol and acetaldehyde-induced tight junction disruption and barrier dysfunction. Pretreatment of cell monolayers with NAC blocked ethanol and acetaldehyde-induced changes in TER, inulin permeability and redistribution of occludin and ZO-1, indicating that oxidative stress plays a role in ethanol and acetaldehyde-induced tight junction disruption and barrier dysfunction. The lack of an effect of DPI indicates that NADPH oxidase does not play a role in ethanol and acetaldehyde-induced oxidative stress and tight junction disruption. Interestingly, CsA blocked ethanol and acetaldehyde-induced changes in TER, inulin permeability and redistribution of occludin and ZO-1, indicating that MMPT and mitochondrial oxidative stress are involved in the synergistic disruption of tight junction and barrier function by ethanol and acetaldehyde in the intestinal epithelium.

In summary, this study provides evidence that ethanol and acetaldehyde synergistically disrupt intestinal epithelial tight junction and induce barrier dysfunction. As illustrated in the figure data indicates the mechanism of synergistic disruption of tight junctions by ethanol and acetaldehyde involves elevation of $[Ca^{2+}]_i$, mitochondrial oxidative stress and activities of Src kinase and MLCK (Fig. 8). This study reveals a new dimension to the role of ethanol metabolism and acetaldehyde production in alcoholic gut permeability and endotoxemia.

Methods

Chemicals. Cell culture supplies, transfection reagents, Fura-2AM and pluronic acid were procured from Cellgro[®] (Manassas, VA) or Invitrogen (Carlsbad, CA). Transwells were purchased from Costar (Cambridge, MA). TPG, ML-7, CsA and PP2 were from EMD Chemicals (San Diego, CA). Other chemicals were purchased from

either Sigma Aldrich (St. Louis, MO) or Thermo Fisher Scientific (Tustin, CA). MitoSOX™ and H₂DCFDA were procured from ThermoFisher:Life Technologies (Grand Island, NY).

Antibodies. Anti-ZO-1 and anti-occludin antibodies were purchased from Invitrogen (Carlsbad, CA). Anti ADH1B and anti-ALDH2 antibodies were procured from Origene Technologies (Atlanta, GA). Anti-TRPV6 antibody was purchased from Santa Cruz Biotechnology (Dallas, TX) and anti-Ca_v1.3 antibody was procured from abcam (Cambridge, MA). HRP-conjugated anti-mouse IgG, HRP-conjugated anti-rabbit IgG and anti-β-actin antibodies were obtained from Sigma Aldrich. AlexaFluor-488-conjugated anti-mouse IgG and Cy3-conjugated anti-rabbit IgG were purchased from Molecular Probes (Eugene, OR).

Expression constructs. ADH1B (SKU: SC335414) and ALDH2 (SKU: MC217268) cDNA in pCMV vector were purchased from Origene (Rockville, MD). A vector-based short hairpin RNA (shRNA) method was used to silence Ca_v1.3 and TRPV6 gene expression in Caco-2 cells. Two targeting sequences each were chosen against the nucleotide sequence of human Ca_v1.3 (Gene ID: 776 CACNAID; NM_000720.2) and human TRPV6 (Gene ID: ECAC2; NM_018646) using Dharmacon siDesigner software: Target 1, CCGAATAGCTCCAAGCAAA (sequence position 290–308) and Target 2, GGAAGACCCAGAGATACA (sequence position 5697–5715) for Ca_v1.3, and Target 1, GACAAAGACTCAGTGGAA (sequence position 2207–2224) and Target 2, GAAACAGCGCTACACATA (sequence position 467–484) for TRPV6. To construct shRNA vectors, two pairs of oligonucleotides containing the antisense sequence, hairpin loop region (TTGATATCCG), and sense sequence with cohesive BamHI and HindIII sites were synthesized (Integrated DNA Technologies Inc., Coralville, IA).

Cell culture and transfection. Caco-2_{bbe2} cells (ATCC, Rockville, MD) were grown under standard cell culture conditions as previously described⁴⁴. Experiments were conducted using cells grown in transwell inserts of varying diameters (6.5 or 12 mm) for 3–4 or 15–17 days.

Cells grown in 6-well costar plates for 24 h showing $\cong 75\%$ confluence were transfected, using 1 ml antibiotics-free DMEM containing 10% FBS, 1 μg DNA plasmid (Empty vector, control or the plasmid DNA carrying the tyrosine mutations), 1 μl Plus reagent, and 3 μl Lipofectamine-R for each well. After 20 hours, the cell monolayers were trypsinized and seeded on to transwell inserts (6.5 mm diameter). Cell monolayers on day 3 or 4 post seeding were used to evaluate the effect of ethanol and acetaldehyde on barrier function.

Cell treatments. Cell monolayers in transwell inserts were incubated with ethanol (0–150 mM), acetaldehyde (100–400 μM) or acetaldehyde (100 or 200 μM) applied 10 min after ethanol (75 mM) treatment as described before¹⁸. In some experiments cell monolayers were pretreated with PP2 (10 μM), ML-7 (1 μM), CsA (20 μM), NAC (10 mM), DPI (1 μM) or Ca²⁺-free medium 50 min prior to ethanol treatment. For Ca²⁺ depletion, Ca²⁺ free medium was prepared in DMEM lacking Ca²⁺. Depletion of [Ca²⁺]_i was achieved by incubation of cells with 10 μM BAPTA-AM or 1 μM TPG for 30 min.

Epithelial barrier function. TER was measured using a Millicell-ERS Electrical Resistance System and macromolecular permeability evaluated by measuring unidirectional flux of FITC-inulin as previously described⁴⁵. The basal TER values for Caco-2 cell monolayers in these experiments were 400–500 Ohms/cm².

Fluorescence microscopy. Caco-2 cell monolayers with 0.2% Triton X-100™, sections were blocked and stained for different proteins as described before⁴⁵. The fluorescence was examined by using a Zeiss LSM 510/710 laser scanning confocal microscope and 20× objective lens. Images from x-y (1 μm) sections were collected using LSM Pascal or Zen software. Images from sections were stacked using ImageJ (NIH) and processed by Adobe Photoshop (Adobe Systems, San Jose, CA).

Measurement of [Ca²⁺]_i. [Ca²⁺]_i was measured as previously described³². Briefly, serum-starved Caco-2 cell monolayers on glass-bottom microwell dishes (MatTek; Ashland, MA) were incubated with Fura-2AM (10 μM) in 0.5% pluronic acid for 30 min. Fura-2-loaded cells were alternately excited at 340 or 380 nm using a PC-driven hyper-switch (Ionoptix; MA, USA). Ratios were collected every second at 510 nm using a Dage MTI iCCD camera and Ionwizard software (Ionoptix). [Ca²⁺]_i was calculated using the following equation: $[Ca^{2+}]_i = K_d (R - R_{min}) (S_{f2}) / (R_{max} - R) (S_{b2})$, where R is the 340/380 nm ratio, R_{min} and R_{max} are the minimum and maximum ratios determined in Ca²⁺-free and saturated Ca²⁺ solutions, respectively, S_{f2}/S_{b2} is the Ca²⁺ free/Ca²⁺-replete ratio of emissions at 380 nm excitation, and K_d is the dissociation constant for Fura-2. R_{min}, R_{max}, S_{f2}, and S_{b2} were determined by increasing the Ca²⁺ permeability of Caco-2 cells with ionomycin (10 μM), and perfusing cells with a high-Ca²⁺ (10 mM) or Ca²⁺-free (10 mM EGTA) solution. The *in situ* apparent dissociation constant (K_d) for Fura-2 used in this study was 224 nM. Eight to ten cells in each monolayer were analyzed simultaneously, and the experiments were repeated in 3–5 monolayers.

Detection of ROS production. Caco-2 monolayers were grown on 60 mm dishes to full confluence. Cell monolayers washed with DMEM without phenol red and were incubated with Hoechst 33342 (1:10000) and 10 μM CM-H₂DCFDA for 40 min at 37 °C in the CO₂ incubator. Following a wash, cells were incubated with 5 mM of MitoSox for 10 min at 37 °C. Cell monolayers were then exposed to osmotic stress, DSS or cyclic stretch for varying times and fluorescence images were captured by confocal microscope. To determine mitochondrial association of ROS cell monolayers were preincubated with 200 nM Mitotracker green for 30 min followed by incubation with 5 mM Mitosox for 10 min at 37 °C and the images captured 30 min.

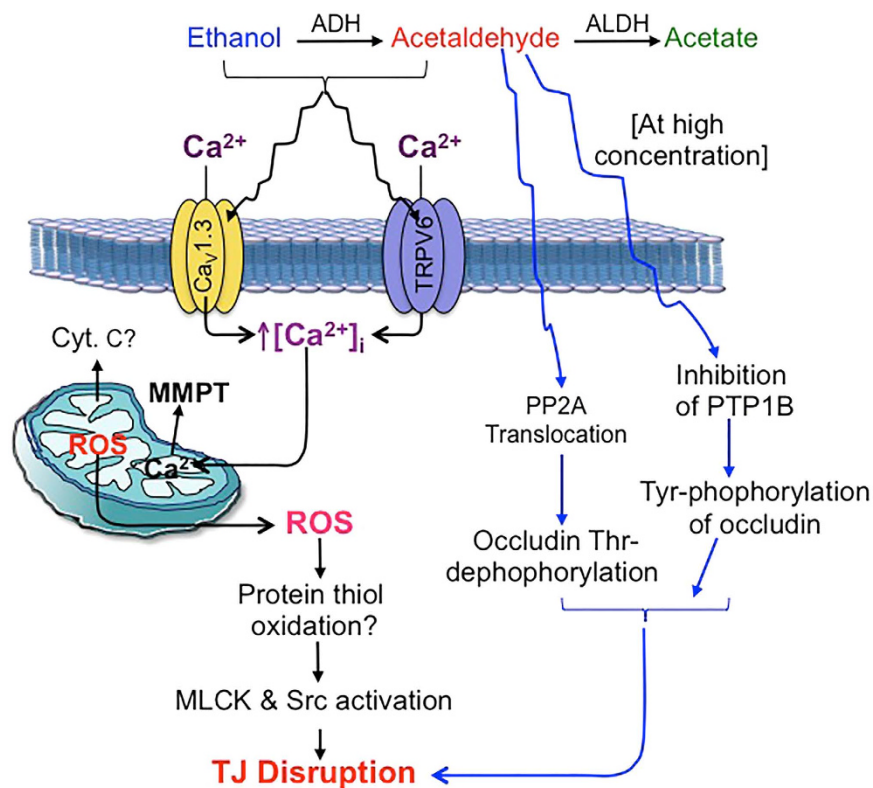


Figure 8. The potential mechanism involved in the synergistic disruption of tight junctions by ethanol and acetaldehyde. At low acetaldehyde concentration (cascade with black arrows on the left), the ethanol and acetaldehyde synergistically elevate $[Ca^{2+}]_i$ in the intestinal epithelium potentially by activating Ca^{2+} channels. Elevated plasma calcium induces oxidative stress likely by causing mitochondrial membrane permeability transition. Oxidative stress-induced protein-thiol oxidation inhibits PTP1B and activates c-Src and MLCK resulting in disruption of epithelial tight junctions. At high acetaldehyde concentration (cascade with blue arrows on the right), it disrupts tight junctions in the absence of ethanol by inhibition of PTP1B leading to Tyr-phosphorylation of occludin and other tight junction proteins, and by translocation of PP2A to tight junction leading to dephosphorylation of occludin on Thr residues.

Immunoblot analysis. Proteins in cell extracts were separated by sodium dodecyl sulfate-polyacrylamide gel (7%) electrophoresis and transferred to polyvinylidene fluoride membranes. Membranes were immunoblotted for different proteins as described before⁴⁵.

NAD/NADH assay. NAD and NADH in cell extracts were measured using Amplitude™ Fluorimetric NAD/NADH ratio assay kit (AAT Bioquest, Inc., Sunnyvale, CA). Cells were extracted using the NAD/NADH lysis buffer and the supernatant was used for assay. NAD and NADH levels were measured according to the procedure provided by the vendor. Protein in extract was measured by BCA method, and NAD/NADH values are calculated as nmole per mg protein.

Statistical analyses. All data are expressed as Mean \pm SEM. The differences among multiple groups were first analyzed by ANOVA. When a statistical significance was detected, Tukey's *t* test was used to determine the statistical significance between multiple testing groups and the corresponding control. Statistical significance was established at 95%.

References

1. Rao, R. Endotoxemia and gut barrier dysfunction in alcoholic liver disease. *Hepatology* **50**, 638–644, doi: 10.1002/hep.23009 (2009).
2. Rao, R. K., Seth, A. & Sheth, P. Recent Advances in Alcoholic Liver Disease I. Role of intestinal permeability and endotoxemia in alcoholic liver disease. *Am J Physiol Gastrointest Liver Physiol* **286**, G881–884, doi: 10.1152/ajpgi.00006.2004286/6/G881 (2004).
3. Tietjen, T. G., Mjaatvedt, C. H. & Yang, V. W. Expression of the class I alcohol dehydrogenase gene in developing rat fetuses. *J Histochem Cytochem* **42**, 745–753 (1994).
4. Kawauchi, S. *et al.* Intestinal and hepatic expression of cytochrome P450s and mdr1a in rats with indomethacin-induced small intestinal ulcers. *Int J Med Sci* **11**, 1208–1217, doi: 10.7150/ijms.9866 (2014).
5. Tillonen, J., Kaihovaara, P., Jousimies-Somer, H., Heine, R. & Salaspuro, M. Role of catalase in *in vitro* acetaldehyde formation by human colonic contents. *Alcohol Clin Exp Res* **22**, 1113–1119 (1998).
6. Seitz, H. K., Bosche, J., Czygan, P., Veith, S. & Kommerell, B. Microsomal ethanol oxidation in the colonic mucosa of the rat. Effect of chronic ethanol ingestion. *Naunyn Schmiedebergs Arch Pharmacol* **320**, 81–84 (1982).

7. Boye, A., Zou, Y. H. & Yang, Y. Metabolic derivatives of alcohol and the molecular culprits of fibro-hepatocarcinogenesis: Allies or enemies? *World J Gastroenterol* **22**, 50–71, doi: 10.3748/wjg.v22.i1.50 (2016).
8. Castro, G. D. *et al.* Acetaldehyde accumulation in rat mammary tissue after an acute treatment with alcohol. *J Appl Toxicol* **28**, 315–321, doi: 10.1002/jat.1281 (2008).
9. Dolai, S. *et al.* Effects of ethanol metabolites on exocytosis of pancreatic acinar cells in rats. *Gastroenterology* **143**, 832–843 e831–837, doi: 10.1053/j.gastro.2012.06.011 (2012).
10. Fang, Z. H., Hu, Y. Y. & Cui, J. W. [Relationship between alcoholic liver injury and endotoxin leakage from gut and intervention effect of jianpi liqi huoxue decoction]. *Zhongguo Zhong Xi Yi Jie He Za Zhi* **26**, 813–817 (2006).
11. Faut, M., Rodriguez de Castro, C., Bietto, F. M., Castro, J. A. & Castro, G. D. Metabolism of ethanol to acetaldehyde and increased susceptibility to oxidative stress could play a role in the ovarian tissue cell injury promoted by alcohol drinking. *Toxicol Ind Health* **25**, 525–538, doi: 10.1177/0748233709345937 (2009).
12. Hu, N., Zhang, Y., Nair, S., Culver, B. W. & Ren, J. Contribution of ALDH2 polymorphism to alcoholism-associated hypertension. *Recent Pat Endocr Metab Immune Drug Discov* **8**, 180–185 (2014).
13. Kaphalia, L., Boroumand, N., Hyunsu, J., Kaphalia, B. S. & Calhoun, W. J. Ethanol metabolism, oxidative stress, and endoplasmic reticulum stress responses in the lungs of hepatic alcohol dehydrogenase deficient deer mice after chronic ethanol feeding. *Toxicol Appl Pharmacol* **277**, 109–117, doi: 10.1016/j.taap.2014.02.018 (2014).
14. Anderson, J. M. & Van Itallie, C. M. Physiology and function of the tight junction. *Cold Spring Harb Perspect Biol* **1**, a002584, doi: 10.1101/cshperspect.a002584 (2009).
15. Shen, L., Weber, C. R., Raleigh, D. R., Yu, D. & Turner, J. R. Tight junction pore and leak pathways: a dynamic duo. *Annu Rev Physiol* **73**, 283–309, doi: 10.1146/annurev-physiol-012110-142150 (2011).
16. Van Itallie, C. M. & Anderson, J. M. Claudin interactions in and out of the tight junction. *Tissue Barriers* **1**, e25247, doi: 10.4161/tisb.25247 (2013).
17. Rao, R. Oxidative stress-induced disruption of epithelial and endothelial tight junctions. *Front Biosci* **13**, 7210–7226 (2008).
18. Atkinson, K. J. & Rao, R. K. Role of protein tyrosine phosphorylation in acetaldehyde-induced disruption of epithelial tight junctions. *Am J Physiol Gastrointest Liver Physiol* **280**, G1280–G1288 (2001).
19. Sheth, P. *et al.* Acetaldehyde dissociates the PTP1B-E-cadherin-beta-catenin complex in Caco-2 cell monolayers by a phosphorylation-dependent mechanism. *Biochem J* **402**, 291–300, doi: 10.1042/BJ20060665 (2007).
20. Dunagan, M., Chaudhry, K., Samak, G. & Rao, R. K. Acetaldehyde disrupts tight junctions in Caco-2 cell monolayers by a protein phosphatase 2A-dependent mechanism. *Am J Physiol Gastrointest Liver Physiol* **303**, G1356–G1364, doi: 10.1152/ajpgi.00526.2011 (2012).
21. Ferrier, L. *et al.* Impairment of the intestinal barrier by ethanol involves enteric microflora and mast cell activation in rodents. *Am J Pathol* **168**, 1148–1154, doi: 10.1016/j.ajcp.2006.04.006 (2006).
22. Chaudhry, K. K. *et al.* ALDH2 Deficiency Promotes Ethanol-Induced Gut Barrier Dysfunction and Fatty Liver in Mice. *Alcohol Clin Exp Res* **39**, 1465–1475, doi: 10.1111/acer.12777 (2015).
23. Ma, T. Y., Nguyen, D., Bui, V., Nguyen, H. & Hoa, N. Ethanol modulation of intestinal epithelial tight junction barrier. *Am J Physiol* **276**, G965–G974 (1999).
24. Rao, R. K. Acetaldehyde-induced increase in paracellular permeability in Caco-2 cell monolayer. *Alcohol Clin Exp Res* **22**, 1724–1730, doi: 00000374-199811000-00015 (1998).
25. Banan, A., Choudhary, S., Zhang, Y., Fields, J. Z. & Keshavarzian, A. Ethanol-induced barrier dysfunction and its prevention by growth factors in human intestinal monolayers: evidence for oxidative and cytoskeletal mechanisms. *The Journal of pharmacology and experimental therapeutics* **291**, 1075–1085 (1999).
26. Banan, A., Fields, J. Z., Decker, H., Zhang, Y. & Keshavarzian, A. Nitric oxide and its metabolites mediate ethanol-induced microtubule disruption and intestinal barrier dysfunction. *The Journal of pharmacology and experimental therapeutics* **294**, 997–1008 (2000).
27. Elamin, E., Masclee, A., Dekker, J. & Jonkers, D. Ethanol disrupts intestinal epithelial tight junction integrity through intracellular calcium-mediated Rho/ROCK activation. *Am J Physiol Gastrointest Liver Physiol* **306**, G677–G685, doi: 10.1152/ajpgi.00236.2013 (2014).
28. Koivisto, T. & Salaspuro, M. Effects of acetaldehyde on brush border enzyme activities in human colon adenocarcinoma cell line Caco-2. *Alcohol Clin Exp Res* **21**, 1599–1605 (1997).
29. Peng, D. K. & Lahann, J. Chemical, electrochemical, and structural stability of low-density self-assembled monolayers. *Langmuir* **23**, 10184–10189, doi: 10.1021/la701660e (2007).
30. Elamin, E. *et al.* Ethanol impairs intestinal barrier function in humans through mitogen activated protein kinase signaling: a combined *in vivo* and *in vitro* approach. *PLoS One* **9**, e107421, doi: 10.1371/journal.pone.0107421 (2014).
31. Basuroy, S. *et al.* Expression of kinase-inactive c-Src delays oxidative stress-induced disassembly and accelerates calcium-mediated reassembly of tight junctions in the Caco-2 cell monolayer. *J Biol Chem* **278**, 11916–11924, doi: 10.1074/jbc.M211710200 (2003).
32. Samak, G., Narayanan, D., Jaggar, J. H. & Rao, R. CaV1.3 channels and intracellular calcium mediate osmotic stress-induced N-terminal c-Jun kinase activation and disruption of tight junctions in Caco-2 CELL MONOLAYERS. *J Biol Chem* **286**, 30232–30243, doi: 10.1074/jbc.M111.240358 (2011).
33. Samak, G. *et al.* Calcium/Ask1/MKK7/JNK2/c-Src signalling cascade mediates disruption of intestinal epithelial tight junctions by dextran sulfate sodium. *Biochem J* **465**, 503–515, doi: 10.1042/BJ20140450 (2015).
34. Elias, B. C. *et al.* Phosphorylation of Tyr-398 and Tyr-402 in occludin prevents its interaction with ZO-1 and destabilizes its assembly at the tight junctions. *J Biol Chem* **284**, 1559–1569, doi: M804783200 10.1074/jbc.M804783200 (2009).
35. Kale, G., Naren, A. P., Sheth, P. & Rao, R. K. Tyrosine phosphorylation of occludin attenuates its interactions with ZO-1, ZO-2, and ZO-3. *Biochem Biophys Res Commun* **302**, 324–329, doi: S0006291X03001670 (2003).
36. He, F. *et al.* Mechanisms of tumor necrosis factor-alpha-induced leaks in intestine epithelial barrier. *Cytokine* **59**, 264–272, doi: 10.1016/j.cyto.2012.04.008 (2012).
37. Marchiando, A. M. *et al.* The epithelial barrier is maintained by *in vivo* tight junction expansion during pathologic intestinal epithelial shedding. *Gastroenterology* **140**, 1208–1218 e1201–1202, doi: 10.1053/j.gastro.2011.01.004 (2011).
38. Samak, G. *et al.* Cyclic stretch disrupts apical junctional complexes in Caco-2 cell monolayers by a JNK-2-, c-Src-, and MLCK-dependent mechanism. *Am J Physiol Gastrointest Liver Physiol* **306**, G947–G958, doi: 10.1152/ajpgi.00396.2013 (2014).
39. Guntaka, S. R., Samak, G., Seth, A., LaRusso, N. F. & Rao, R. Epidermal growth factor protects the apical junctional complexes from hydrogen peroxide in bile duct epithelium. *Lab Invest* **91**, 1396–1409, doi: 10.1038/labinvest.2011.73 (2011).
40. Peng, T. I. & Jou, M. J. Oxidative stress caused by mitochondrial calcium overload. *Ann N Y Acad Sci* **1201**, 183–188, doi: 10.1111/j.1749-6632.2010.05634.x (2010).
41. Mukhopadhyay, P., Rajesh, M., Yoshihiro, K., Hasko, G. & Pacher, P. Simple quantitative detection of mitochondrial superoxide production in live cells. *Biochem Biophys Res Commun* **358**, 203–208, doi: 10.1016/j.bbrc.2007.04.106 (2007).
42. Wang, H. & Joseph, J. A. Quantifying cellular oxidative stress by dichlorofluorescein assay using microplate reader. *Free Radic Biol Med* **27**, 612–616 (1999).
43. Bernardi, P., Broekemeier, K. M. & Pfeiffer, D. R. Recent progress on regulation of the mitochondrial permeability transition pore; a cyclosporin-sensitive pore in the inner mitochondrial membrane. *J Bioenerg Biomembr* **26**, 509–517 (1994).

44. Rao, R. K., Basuroy, S., Rao, V. U., Karnaky, K. J. Jr. & Gupta, A. Tyrosine phosphorylation and dissociation of occludin-ZO-1 and E-cadherin-beta-catenin complexes from the cytoskeleton by oxidative stress. *Biochem J* **368**, 471–481, doi: 10.1042/BJ20011804 (2002).
45. Samak, G., Suzuki, T., Bhargava, A. & Rao, R. K. c-Jun NH2-terminal kinase-2 mediates osmotic stress-induced tight junction disruption in the intestinal epithelium. *Am J Physiol Gastrointest Liver Physiol* **299**, G572–584, doi: 10.1152/ajpgi.00265.2010 (2010).

Acknowledgements

This study was supported by National Institute of Health grants R01-AA12307 and R01-DK55532.

Author Contributions

Dr. Samak performed initial experiments and was involved in data analysis and organization and preparing results and Methods section of the manuscript. Dr. Meena performed experiments related to calcium channel and oxidative stress. Dr. Gangwar performed experiments related to calcium channel and oxidative stress and data organization. Mr. Roshan Rao performed experiments related to calcium depletion and tight junction regulation. Dr. Pradeep Shukla performed experiments related to shRNA transfection. Ms. Bhargavi Manda participated in immunofluorescence staining of cell monolayers. Dr. Narayanan's contribution includes conducting calcium measurement experiments and data processing and organization. Dr. Jaggar has contributed to this study by design of calcium measurement experiments, data interpretation and editing the manuscript. Dr. R.K. Rao is responsible for the design of experiments, interpretation of data and manuscript writing.

Additional Information

Supplementary information accompanies this paper at <http://www.nature.com/srep>

Competing financial interests: The authors declare no competing financial interests.

How to cite this article: Samak, G. *et al.* Calcium Channels and Oxidative Stress Mediate a Synergistic Disruption of Tight Junctions by Ethanol and Acetaldehyde in Caco-2 Cell Monolayers. *Sci. Rep.* **6**, 38899; doi: 10.1038/srep38899 (2016).

Publisher's note: Springer Nature remains neutral with regard to jurisdictional claims in published maps and institutional affiliations.



This work is licensed under a Creative Commons Attribution 4.0 International License. The images or other third party material in this article are included in the article's Creative Commons license, unless indicated otherwise in the credit line; if the material is not included under the Creative Commons license, users will need to obtain permission from the license holder to reproduce the material. To view a copy of this license, visit <http://creativecommons.org/licenses/by/4.0/>

© The Author(s) 2016